

The combined influence of the stratospheric polar vortex and ENSO on zonal asymmetries in the Southern Hemisphere upper tropospheric circulation during austral spring and summer

Article

Supplemental Material

Osman, M., Shepherd, T. G. ORCID: <https://orcid.org/0000-0002-6631-9968> and Vera, C. S. (2022) The combined influence of the stratospheric polar vortex and ENSO on zonal asymmetries in the Southern Hemisphere upper tropospheric circulation during austral spring and summer. *Climate Dynamics*, 59 (9-10). pp. 2949-2964. ISSN 1432-0894 doi: 10.1007/s00382-022-06225-0 Available at <https://centaur.reading.ac.uk/104127/>

It is advisable to refer to the publisher's version if you intend to cite from the work. See [Guidance on citing](#).

To link to this article DOI: <http://dx.doi.org/10.1007/s00382-022-06225-0>

Publisher: Springer

including copyright law. Copyright and IPR is retained by the creators or other copyright holders. Terms and conditions for use of this material are defined in the [End User Agreement](#).

www.reading.ac.uk/centaur

CentAUR

Central Archive at the University of Reading

Reading's research outputs online

1 The Combined Influence of the Stratospheric Polar Vortex and
2 ENSO on Zonal Asymmetries in the Southern Hemisphere Upper
3 Tropospheric Circulation during Austral Spring and Summer:
4 Supplementary material

5 Marisol Osman

Theodore G. Shepherd

Carolina S. Vera

6 April 26, 2021

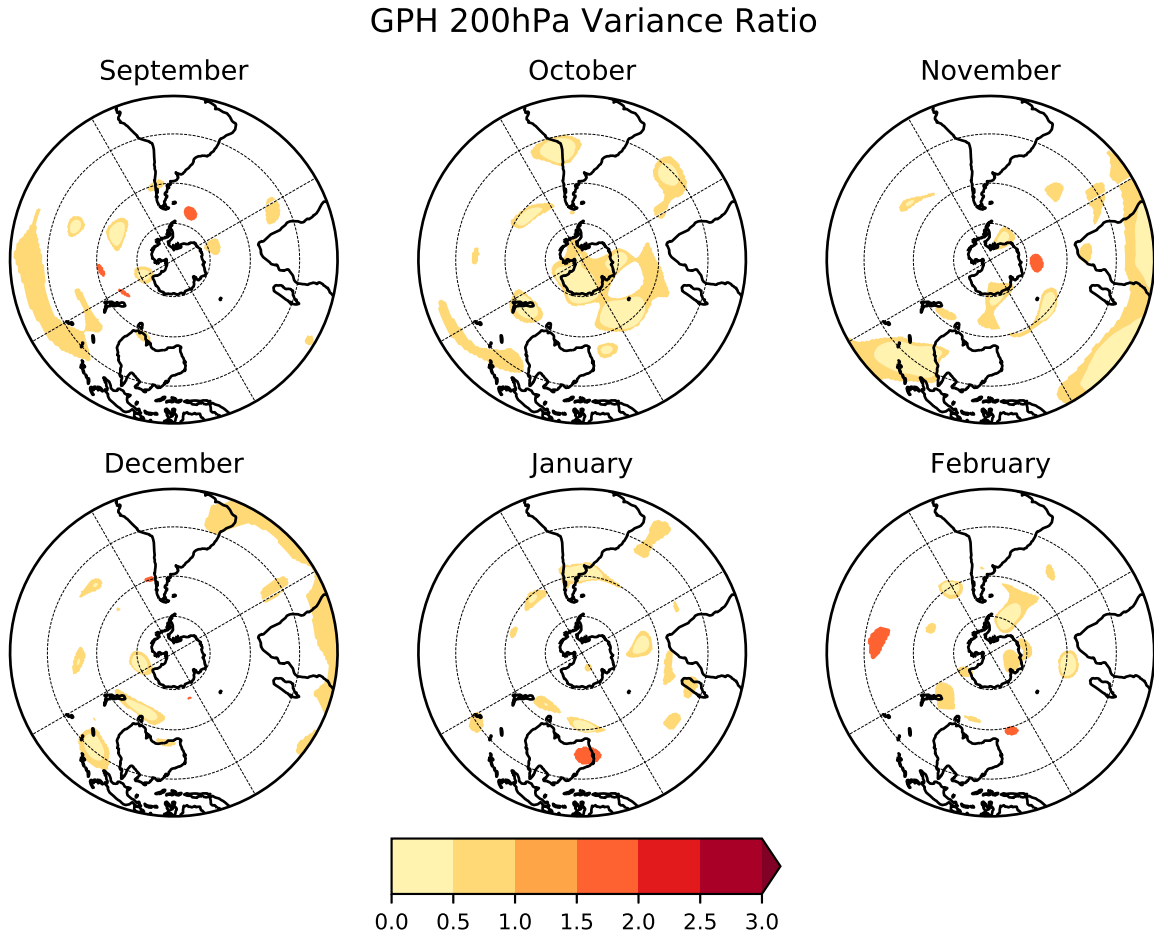


Figure S1: Ratio of climatological variance of Z at 200hPa between hindcasts and ERA-Interim for (a) September, (b) October, (c) November, (d) December, (e) January, (f) February 1981-2018. The year 2002 has been excluded. Coloured regions indicate differences that are statistically different at the 5% level based on a two-sided chi-square test. Hindcasts initialized on 1 August.

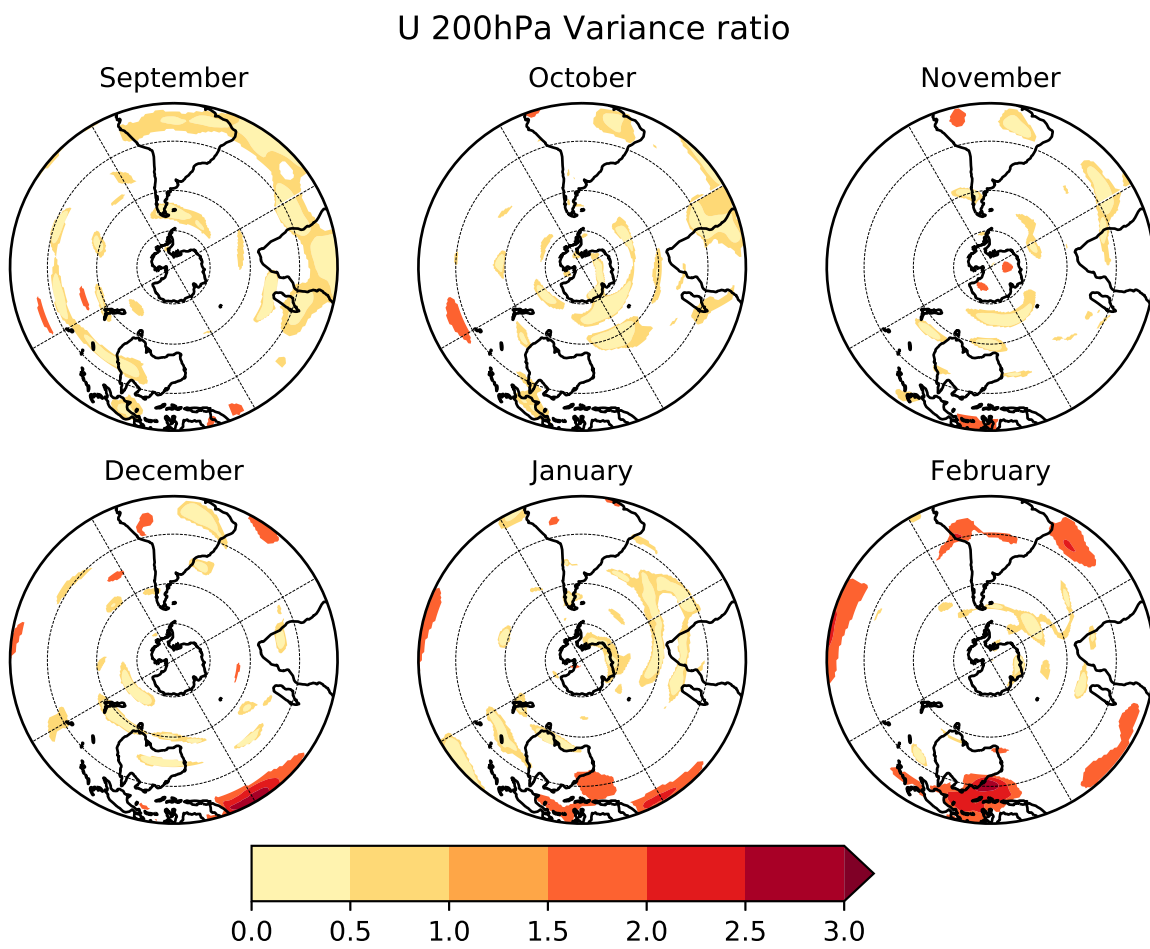


Figure S2: Same as Fig. S1 but for zonal wind u .

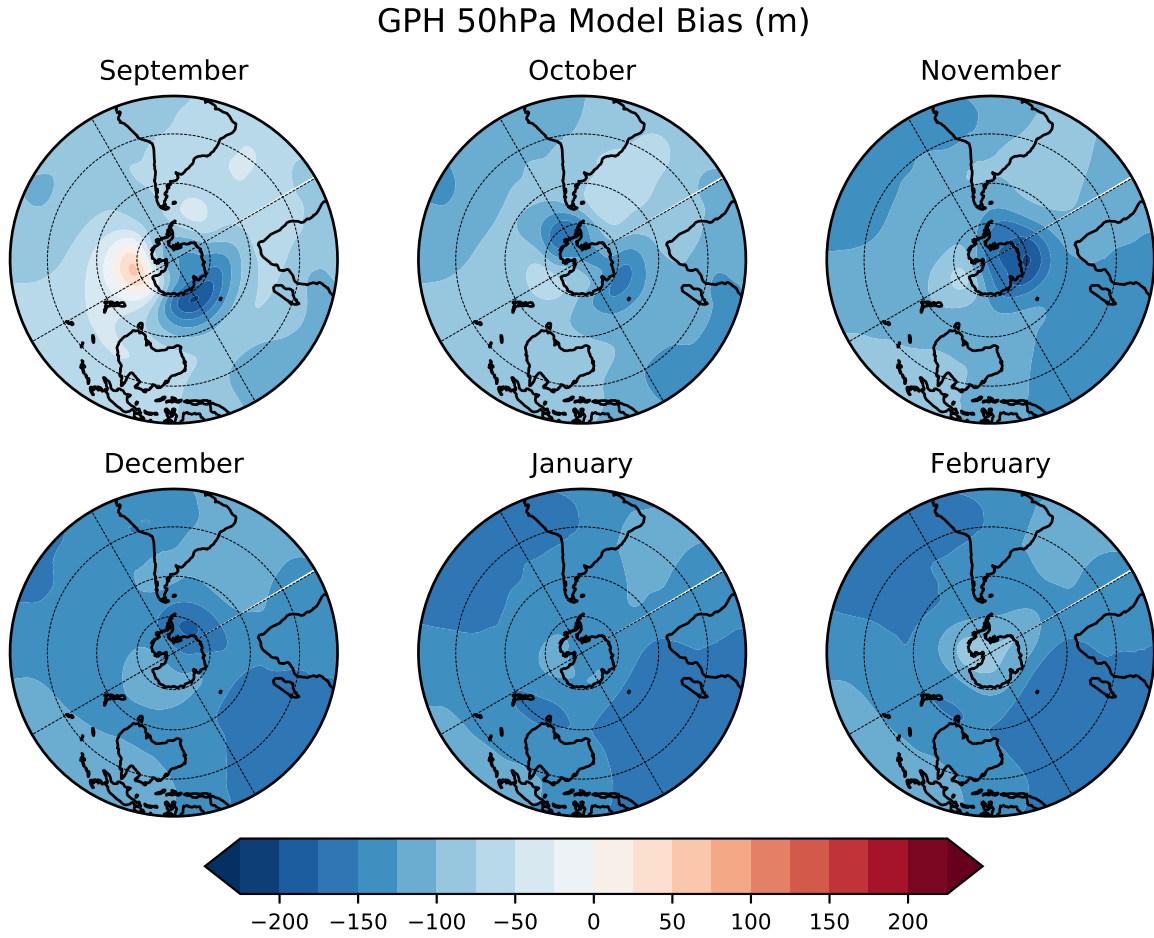


Figure S3: Monthly mean climatological differences in Z at 50hPa between hindcasts and ERA-Interim (m) for (a) September, (b) October, (c) November, (d) December, (e) January, (f) February 1981-2018. The year 2002 has been excluded. Coloured regions indicate differences that are statistically different at the 5% level based on a two-sided t-test. Hindcasts initialized on 1 August.

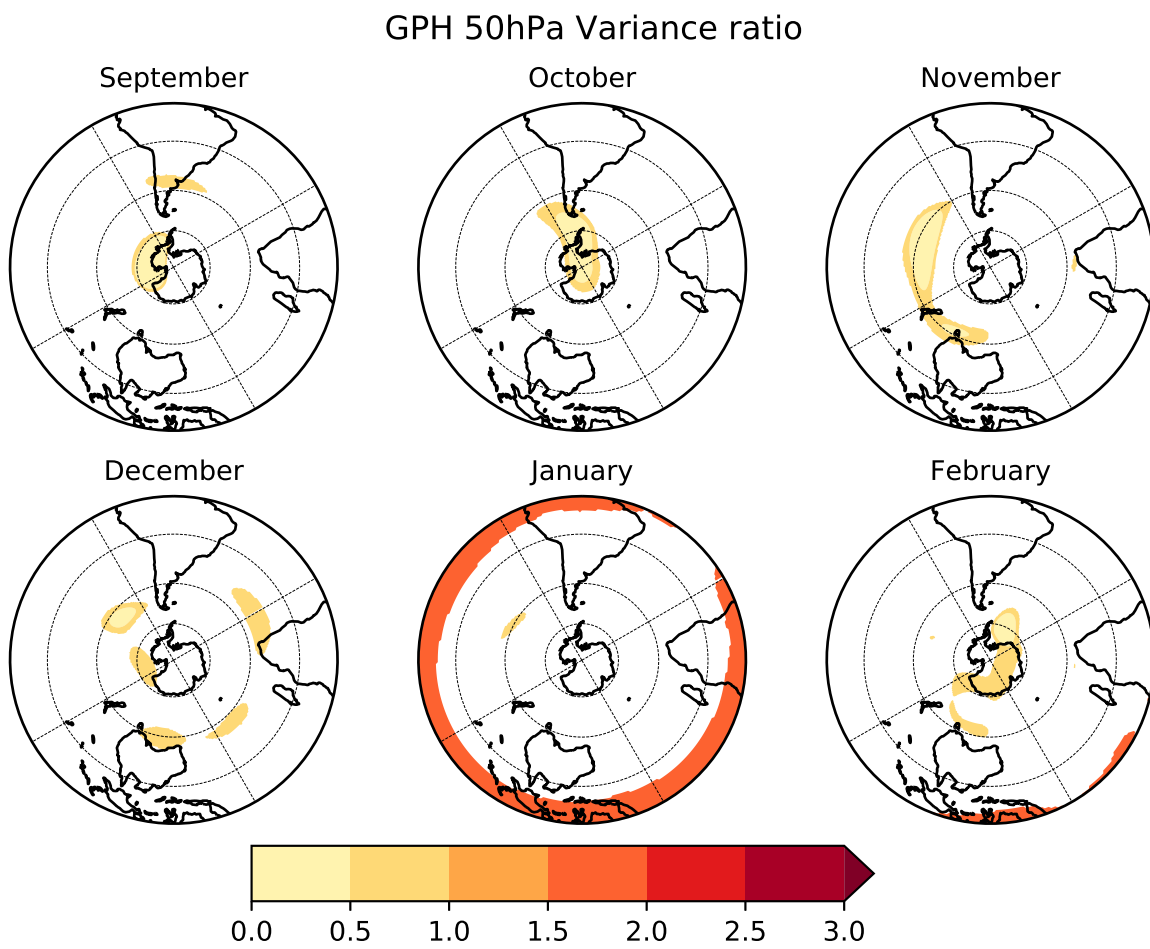


Figure S4: Same as Fig. S1 but for Z at 50hPa.

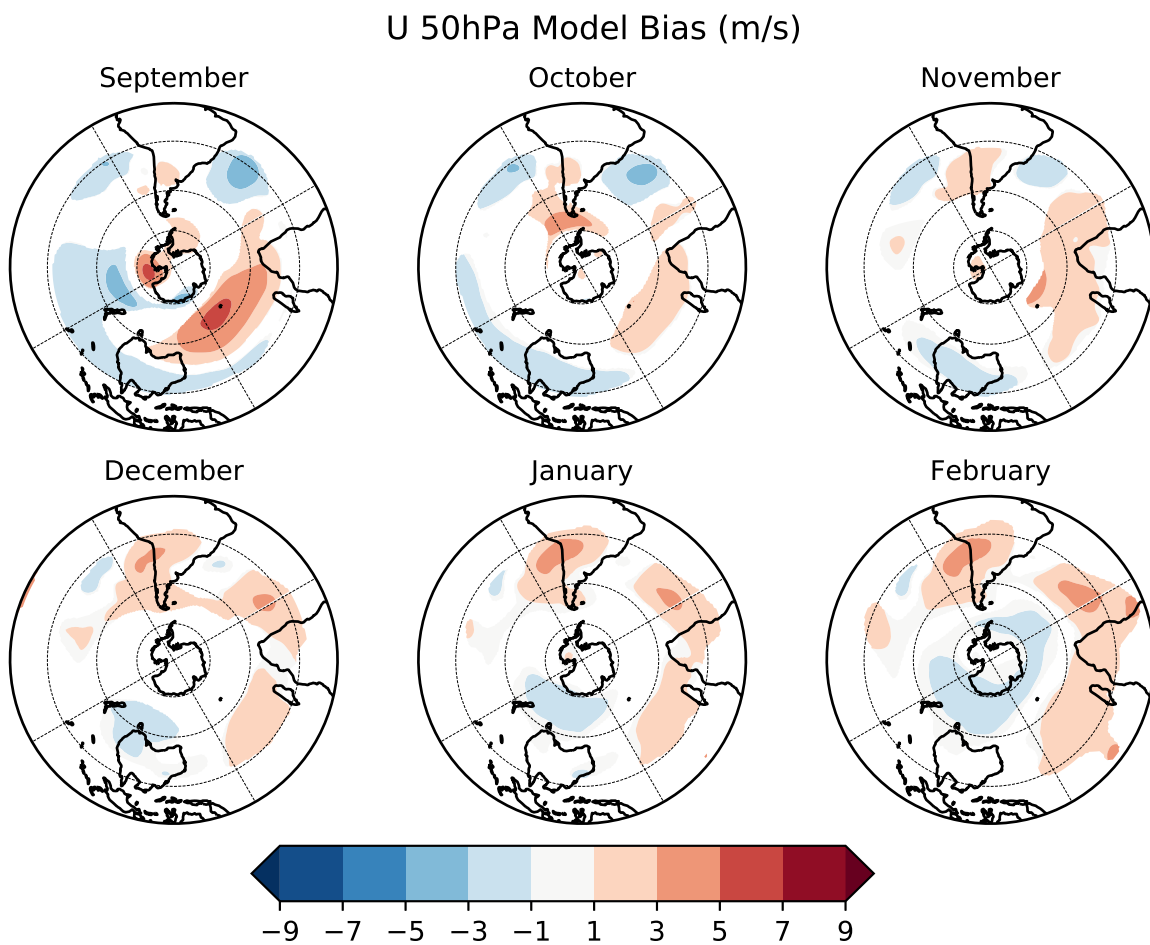


Figure S5: Same as Fig. S3 but for zonal wind u .

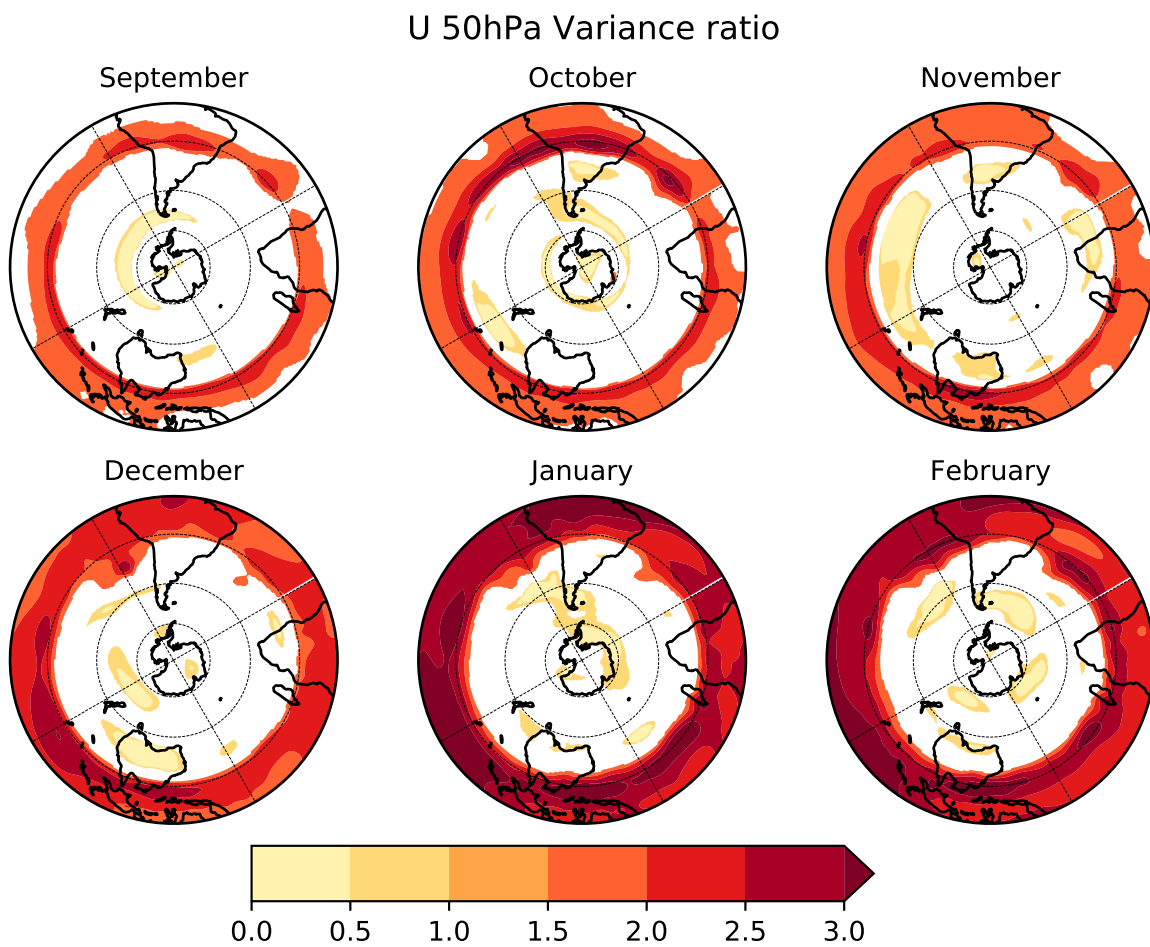


Figure S6: Same as Fig. S2 but for zonal wind u at 50hPa.

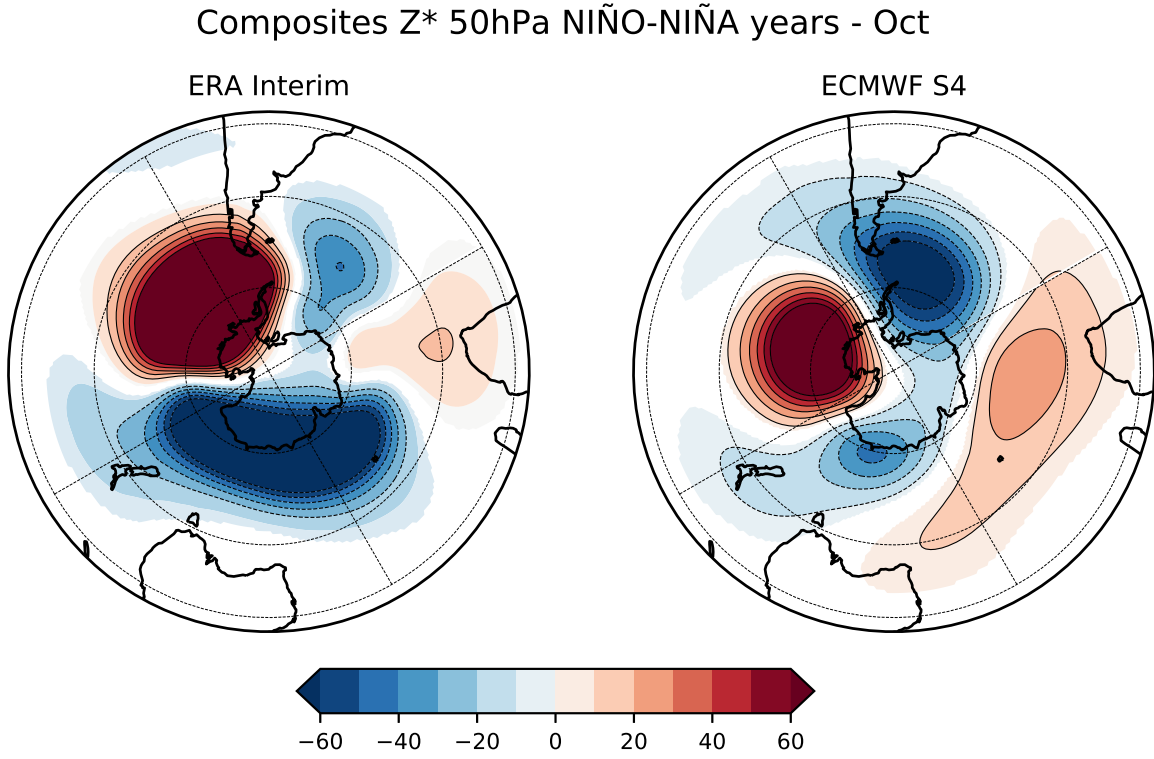


Figure S7: Composite differences of Z^* at 50hPa between El Niño and La Niña in October for (a) ERA-Interim and (b) hindcasts. Units are in m and coloured regions are statistically different from zero at the 5% level based on a t-test.

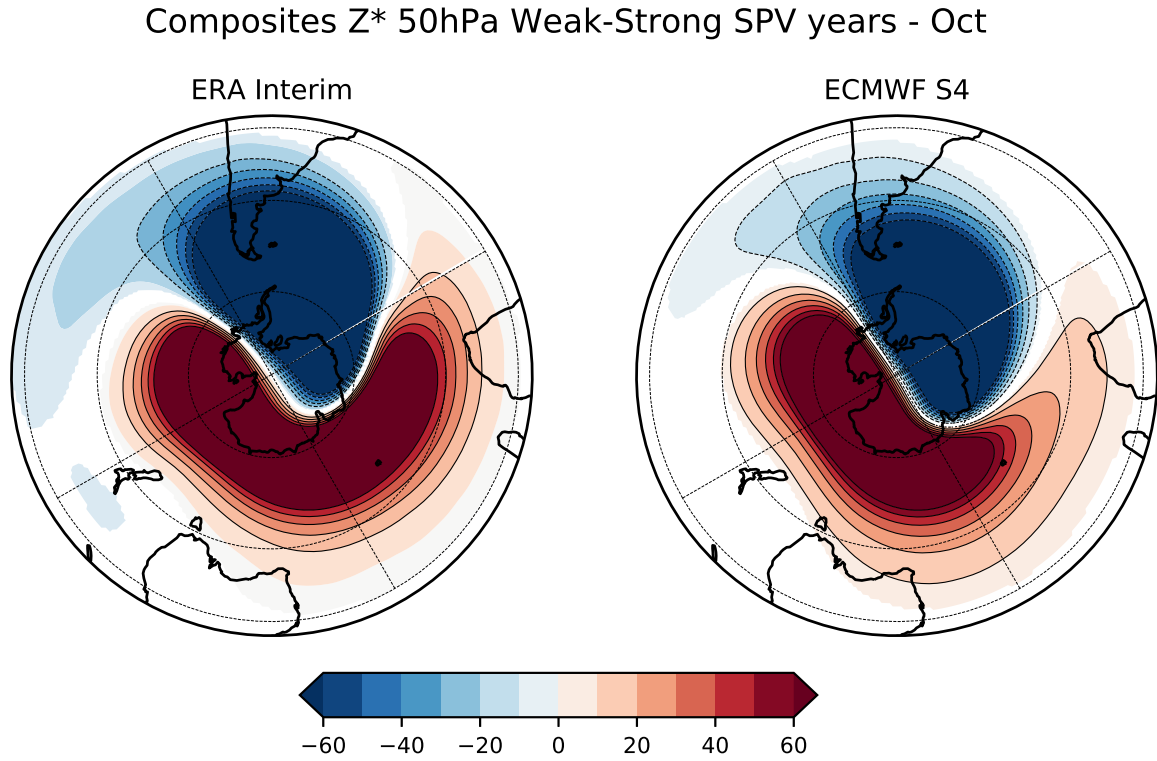


Figure S8: Composite differences of Z^* at 50hPa between weak and strong SPV in October for (a) ERA-Interim and (b) hindcasts. Units are in m and coloured regions are statistically different from zero at the 5% level based on a t-test.

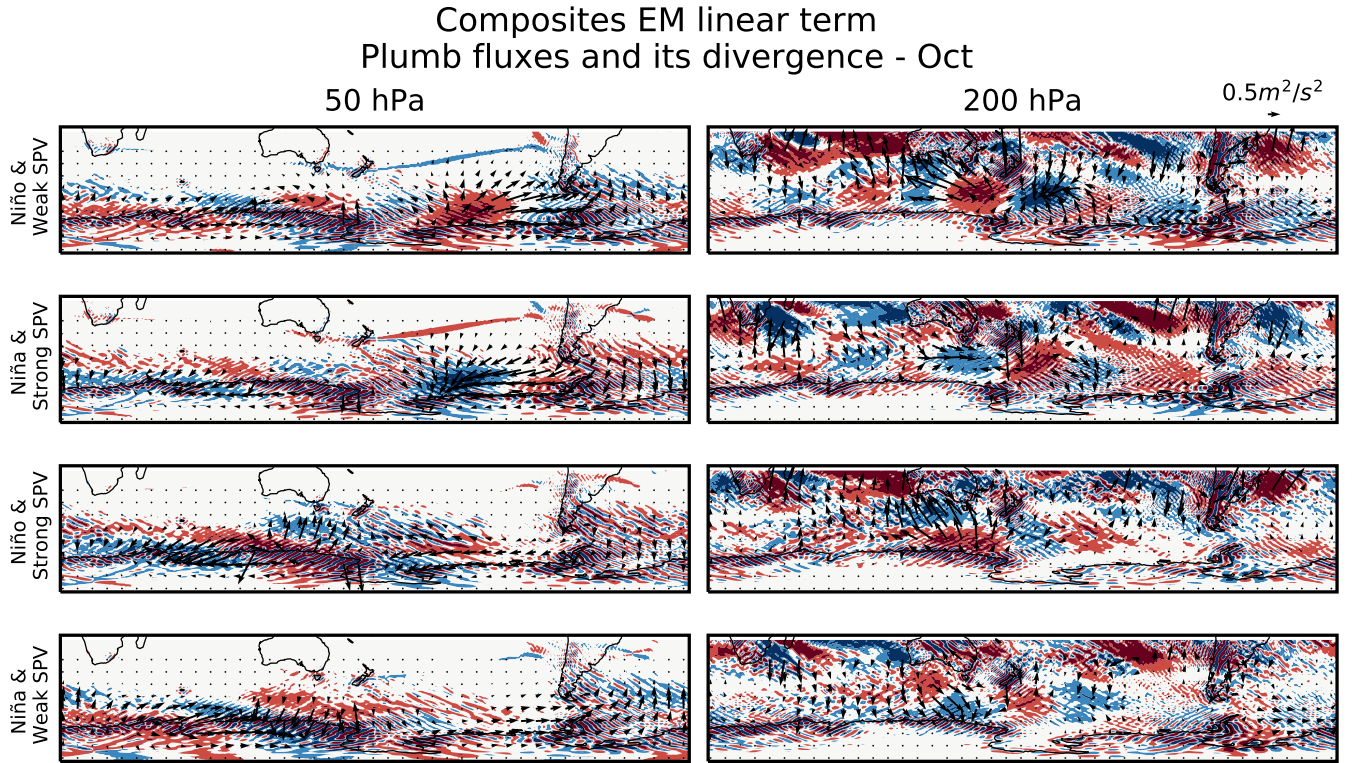


Figure S9: Linear term of the ensemble mean response of the wave activity flux response (arrows) and its divergence (shaded) at 50hPa (left column) and 200hPa (right column) to in-phase and out-of-phase events. Convergence (divergence) levels are $\pm 0.3e-6ms^{-2}$ and $\pm 1e-6ms^{-2}$.

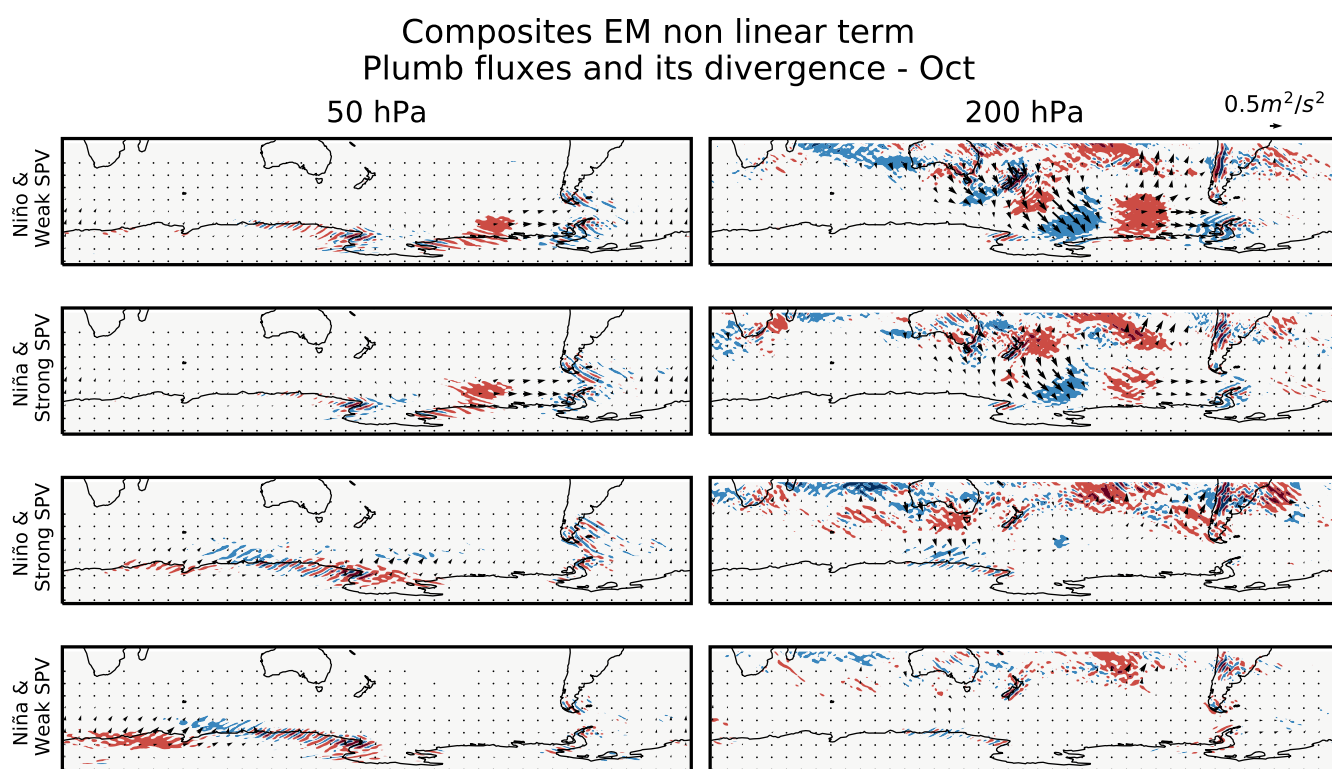


Figure S10: Same as Fig. S9 but for the non-linear term of the ensemble mean response.